

000 001 002 003 004 005 006 007 008 009 010 011 012 013 014 015 016 017 018 019 020 021 022 023 024 025 026 027 028 029 030 031 032 033 034 035 036 037 038 039 040 041 042 043 044 045 046 047 048 049 050 051 052 053 HOW NOT TO BENCHMARK YOUR SITE METRIC: BE- YOND STATIC LEADERBOARDS AND TOWARDS REALIS- TIC EVALUATION.

Anonymous authors

Paper under double-blind review

ABSTRACT

Transferability estimation metrics are used to find a high-performing pre-trained model for a given target task without fine-tuning the models and without access to the source dataset. Despite the growing interest in developing such metrics, the benchmarks used to measure their progress have largely gone unexamined. In this work, we empirically show the shortcomings of widely used benchmark setups for evaluating transferability estimation metrics. We argue that the benchmarks on which these metrics are evaluated are fundamentally flawed. We empirically demonstrate that their unrealistic model spaces and static performance hierarchies artificially inflate the perceived performance of existing metrics to the point where simple, dataset-agnostic heuristics can outperform sophisticated methods. Our analysis reveals a critical disconnect between current evaluation protocols and the complexities of real-world model selection. To address this, we provide concrete recommendations for constructing more robust and realistic benchmarks to guide future research in a more meaningful direction as well as provide a benchmark based on the proposed best practices for vision classification.

1 INTRODUCTION

Using models that are pre-trained on large datasets like ImageNet (Deng et al., 2009) has become standard practice in real-world deep-learning scenarios. However, performance gains can vary considerably depending on the model architecture, weights, and the dataset on which it was pre-trained (the source dataset). This leads to the pre-trained model selection problem. This raises the question: *“How can we find a high-performing pre-trained model for a given target task without fine-tuning our models and without access to the source dataset.”* Source Independent Transferability Estimation (SITE) metrics address this question by computing a cheap-to-calculate score for each candidate model, that is used to rank models by their predicted downstream performance. This research area is growing rapidly, with papers appearing at major AI venues such as ICML, NeurIPS, and CVPR. Progress in the field has so far been measured primarily against a small set of widely adopted benchmarks.

While these benchmarks have been useful for driving early advances, we argue that they fail to capture the complexities of real-world applications. To address this gap, our paper offers a critical empirical analysis of the most commonly used benchmark setup for SITE metric evaluation. We identify fundamental flaws in its design that call into question the validity of reported results. Our contributions are to:

1. Empirically demonstrate how current benchmarking practices give misleading performances of SITE metrics which questions their reliability,
2. Show that a simple, static ranking heuristic can outperform sophisticated metrics, exposing the trivial nature of the task posed by the benchmark which further highlights the weakness of the current benchmark, and
3. Propose a set of actionable best practices for constructing more robust and meaningful benchmarks suitable for practical challenges of real-world model selection.

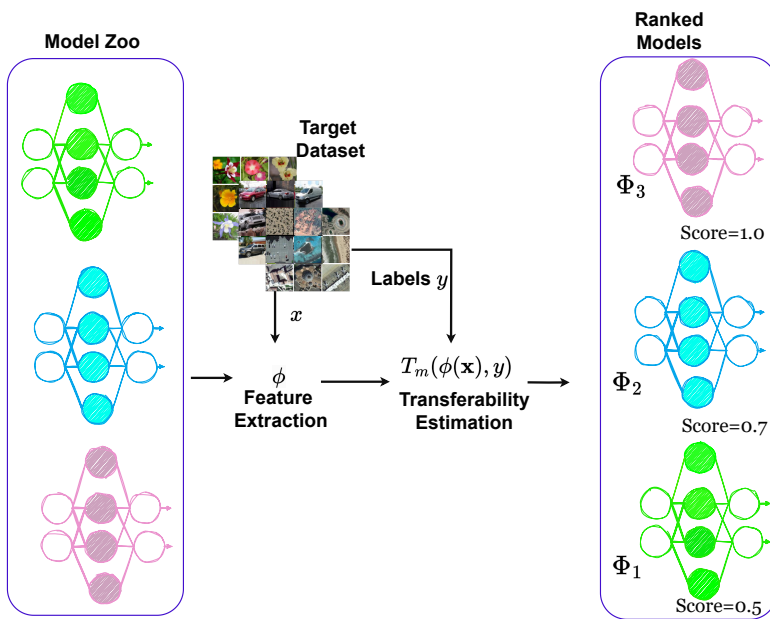


Figure 1: Illustration of Source Independent Transferability Estimation (SITE): Given a set of pre-trained models (on the left), a SITE metric computes a score T_m based on extracted features on a target dataset. The scores T_m are used to rank the pre-trained models according to their transferability.

Despite significant progress in the development of novel SITE methods, the empirical evaluation standards within this emerging research area have yet to reach the maturity seen in other machine learning domains. To address this issue, we propose best practices to rectify them, leading to the SITE benchmarking and evaluation checklist (Appendix A).

2 TRANSFERABILITY ESTIMATION: BACKGROUND

The idea behind transferability estimation is simple: estimate which model from a zoo of models would perform best after fine-tuning. Transferability estimation as a research area is fairly young; the H-Score (Bao et al., 2019) and NCE (Tran et al., 2019) can be considered early works on this topic, introducing the evaluation of transferability and the assignment of models corresponding to an estimate of their transferability for a given target task. We illustrate how transferability estimation metrics work in Figure 1.

There are two widely accepted problem scenarios for transferability estimation: source-dependent transferability estimation (where one has access to the source and target dataset) and source-independent transferability estimation (where one does not have access to the source dataset), we will be focusing on the latter.

2.1 SOURCE DEPENDENT TRANSFERABILITY ESTIMATION (SDTE)

The SDTE scenario assumes access to the source datasets on which the models have been pre-trained. Apart from the fact that this assumption is often not met, a drawback of common SDTE metrics is the use of distribution matching methods like optimal transport (Tan et al., 2021), which are typically very expensive to compute. In addition, SDTE metrics are not reliable when the discrepancy between the source and target datasets is very high (Braccajoli et al., 2025); for example, when comparing the entire ImageNet21K (Deng et al., 2009) to the Cars (Krause et al., 2013) or Plants (G. & J., 2019) datasets.

108
109

2.2 SOURCE INDEPENDENT TRANSFERABILITY ESTIMATION (SITE)

110
111
112
113
114
115
116
117
118
119
120
121
122
123
124
125
126
127
128
129
130
131

The Source Independent Transferability Estimation (SITE) assumes access to the source model but not the source training data. This is a more realistic scenario, as we might not always have access to the source dataset, nor have the capacity to store the typically very large source datasets like ImageNet (Deng et al., 2009) or LAION (Schuhmann et al., 2022) in our local setup. SITE methods typically rely on evaluating the feature representation of the source model on the target dataset and its relationship with the target labels. There are several SITE metrics inspired by various viewpoints. For instance, LogME (You et al., 2021) formalizes the transferability estimation as the maximum label marginalized likelihood and adopts a directed graphical model to solve it. SFDA (Shao et al., 2022) proposes a self-challenging mechanism; it first maps the features and then calculates the sum of log-likelihood as the metric. ETran (Gholami et al., 2023) and PED (Li et al., 2023) treat the problem of SITE with an energy function and act as a pre-processor for other SITE methods. ETran uses energy-based models to detect whether a target dataset is in-distribution or out of distribution for a given pre-trained model, whereas PED utilizes a potential energy function to modify feature representations to aid other transferability metrics like LogME and SFDA. LEEP (Nguyen et al., 2020) is the average log-likelihood of the log-expected empirical predictor, which is a non-parametric classifier based on the joint distribution of the source and target distribution. N-LEEP (Li et al., 2021) is a further improvement on LEEP by substituting the output layer with a Gaussian mixture model. TransRate (Huang et al., 2022) treats SITE from an information theory point of view by measuring the transferability as the mutual information between features of target examples extracted by a pre-trained model and their labels. There have been applications of transferability estimation and proposed metrics for different domains such as medical imaging (Juodelyte et al., 2024; Singh et al., 2025; Yang et al., 2023) and speech recognition (Chen et al., 2023). We suggest the survey by Ding et al. (2024) for a complete view of transferability metrics.

132
133

3 SITE: PROBLEM STATEMENT

134
135
136
137
138
139
140
141
142
143

We assume that we are given a target dataset $\mathcal{D} = \{(\mathbf{x}_n, y_n)\}_{n=1}^N$ of N labeled points and M pre-trained models $\{\Phi_m = (\phi_m, \psi_m)\}_{m=1}^M$. Each model Φ_m consists of a feature extractor $\phi_m(x) \in \mathbb{R}^d$ that returns a d -dimensional embedding and the final layer or head ψ_m that outputs the label prediction for the given input $\phi_m(x)$. The task of estimating transferability is to generate a score for each pre-trained model so that the best model is at the top of a ranking list. For each pre-trained model Φ_m , a transferability metric outputs a scalar score T_m that should be coherent in its ranking with the performance of the fine-tuned classifier $\hat{\Phi}_m$. That is, the goal is to obtain scores such that score $T_{\textcolor{blue}{m}_1} \geq T_{\textcolor{blue}{m}_2}$ if and only if the fine-tuned model $\hat{\Phi}_{\textcolor{blue}{m}_1}$ has a higher probability to predict the correct labels on the target dataset than model $\hat{\Phi}_{\textcolor{blue}{m}_2}$:

144
145
146

$$\frac{1}{N} \sum_{n=1}^N p(y_n | \mathbf{x}_n; \hat{\Phi}_{\textcolor{blue}{m}_1}) \geq \frac{1}{N} \sum_{n=1}^N p(y_n | \mathbf{x}_n; \hat{\Phi}_{\textcolor{blue}{m}_2}),$$

147
148
149
150

where $p(y_n | \mathbf{x}_n; \hat{\Phi}_m)$ indicates the probability that the fine-tuned model $\hat{\Phi}_m$ predicts label y_n for input \mathbf{x}_n . Hence, a larger T_m should correspond to a better performance of the model on target data \mathcal{D} .

151

4 TRANSFERABILITY ESTIMATION: STANDARD SETUP

152
153
154
155
156
157

Widely adopted transferability estimation methods, such as LogME (You et al., 2021), TransRate (Huang et al., 2022), NCTI (Wang et al., 2023), LEEP (Nguyen et al., 2020), SFDA (Shao et al., 2022), ETran (Gholami et al., 2023), GBC (Pándy et al., 2022) and LEAD (Hu et al., 2024) are evaluated on benchmarks sharing similar models and datasets.

158
159
160
161

The setup used in LogME, TransRate, H-Score, SFDA, ETran, and NCTI uses pre-trained ResNets (He et al., 2015) (ResNet34, ResNet50, ResNet101, ResNet151), DenseNets (Huang et al., 2016) (DenseNet169, DenseNet121, DenseNet201), MobileNet (Howard et al., 2017), Inceptionv3 (Szegedy et al., 2015), MNASNet (Tan et al., 2018) and GoogleNet (Szegedy et al., 2014). These models are fine-tuned on CIFAR10 (Krizhevsky et al., 2009), CIFAR100 (Krizhevsky et al., 2009), Pets (Parkhi

162 et al., 2012), Aircraft (Maji et al., 2013a), Food (Bossard et al., 2014) and DTD (Cimpoi et al., 2014).
 163 In this work, we focus on this widely adopted SITE benchmark setup.

164 **Fine-tuning details**

166 To obtain test accuracies, these models were fine-tuned with a grid search over learning rates
 167 $\{10^{-1}, 10^{-2}, 10^{-3}, 10^{-4}\}$ and a weight decay in $\{10^{-3}, 10^{-4}, 10^{-5}, 10^{-6}, 0\}$. The best hyperpa-
 168 rameters are determined based on the validation set. The final model is fine-tuned on the target
 169 dataset with the selected parameters. The resulting test accuracy is used as the ground truth score
 170 G_m for model Φ_m . This way, we obtain a set of scores $\{G_m\}_{m=1}^M$ as the ground truth to evaluate our
 171 pre-trained model rankings.

172 **Evaluation Protocol**

174 The evaluation of transferability metrics reflects the correlation between the ground truth accuracy
 175 and the achieved SITE score. Currently, weighted Kendall's Tau (Vigna, 2015) prevails as a measure
 176 to estimate the correlation. Earlier transferability works like H-score used Pearson correlation as
 177 an evaluation metric, but Pearson's r is considered as too sensitive to scale, as two scorings will
 178 induce the same order can differ in their evaluation merely due to calibration. Kendall's τ is a more
 179 interpretable rank statistic, as it counts the number of swaps that bubble sort would have to perform
 180 to put one list in the same order as the other one. More precisely, Kendall's τ returns the ratio of
 181 concordant pairs minus discordant pairs when enumerating all pairs of transferability estimations
 $\{T_m\}_{m=1}^M$ and ground truth transferability scores $\{G_m\}_{m=1}^M$, as given by:

$$\tau = \frac{2}{M(M-1)} \sum_{1 \leq i < j \leq M} \text{sgn}(G_i - G_j) \text{sgn}(T_i - T_j).$$

185 The sgn function returns the sign of the input value and zero if the input value is zero. Since practical
 186 applications rely mainly on the correct order for the top performing pre-trained models, a weighted
 187 variant of Kendall's τ_w is used. Weighted Kendall's τ_w is computed as

$$\tau_w = \frac{2}{M(M-1)} \sum_{1 \leq i < j \leq M} \text{sgn}(G_i - G_j) \text{sgn}(T_i - T_j) w(\rho(i), \rho(j)),$$

191 where $\rho(i)$ returns a ranking of indices, starting at zero. As a default choice, weighted Kendall's tau
 192 uses hyperbolic weighing: $w(r, s) = \frac{1}{s+1} + \frac{1}{r+1}$. In transferability estimation, the ranking ρ reflects
 193 the ranking of the ground truth accuracy. As a result, any pair that involves one of the top transferring
 194 models gets a large weight. In the rest of the text, we will refer to this benchmark (datasets, models,
 195 evaluation protocol) as *standard benchmark*.

196 **5 AN EMPIRICAL CRITIQUE OF THE STANDARD BENCHMARK**

199 While the standard benchmark is widely used, we contend that it is built on flawed foundations
 200 that lead to an overestimation of the true capabilities of SITE metrics. We identify and empirically
 201 validate three critical limitations: an unrealistic model space that does not reflect practical challenges
 202 in transferability estimation, a benchmark that is solved by a static ranking for all considered datasets,
 203 and misleading differences in SITE scores that do not meaningfully correlate with performance
 204 gaps. For the purpose of this study, we examine the following metrics on the standard benchmark:
 205 LogME (You et al., 2021), TransRate (Huang et al., 2022), GBC (Pády et al., 2022), NLEEP (Li
 206 et al., 2021), (Shao et al., 2022), and H-Score (Bao et al., 2019)

207 **5.1 CRITIQUE 1: THE MODEL SEARCH SPACE IS UNREALISTIC**

209 We argue that the model space of the standard benchmark's model pool is **unrealistic**, because it is
 210 dominated by models of varying sizes from only two architectural families (ResNets and DenseNets).
 211 In a real-world scenario, practitioners are not interested in knowing whether they should use a "bigger
 212 vs. smaller" ResNet, but rather which architecture performs **under particular constraints such as size ,**
213 training speed, inference speed, and ease of access. For example, larger **vision classification** models
 214 are known to predictably outperform their shallower counterparts (He et al., 2015), and mixing small
 215 and large variants of the same family of **vision classification** models reduces the complex task of
 model selection to a trivial detection of the largest model.

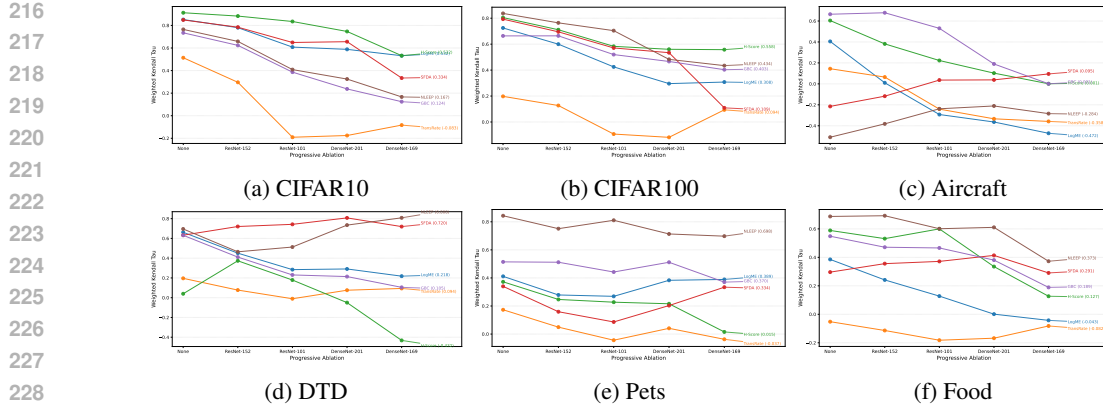


Figure 2: Performance of transferability metrics when we remove architectures of the same families. We sequentially remove the architectures denoted on the horizontal axis and report the achieved τ_w . A pattern of performance decrease with every ablation is observed.

The inclusion of MobileNet and MNASNet alongside ResNets and DenseNets is likewise misaligned with the benchmark’s use case. MobileNet and MNASNet are designed for edge computing environments. In the experimental evaluation, MobileNet and MNASNet consistently occupy the bottom ranks (cf. Figure 3). Hence, removing those models from the search space has little effect on the performance evaluation. However, we advocate against using these models in the standard benchmark to avoid unnecessary inflation of the search space.

We therefore recommend (i) excluding edge-oriented models from the benchmark and (ii) using at most one representative architecture per family, ensuring that the compared models have similar sizes.

Validation via Model Ablation To test the robustness of SITE metrics under a more realistic search space, we ablate the largest models from overrepresented families (ResNet-152, ResNet-101, DenseNet-169, DenseNet-201) and recompute weighted Kendall’s τ_w . Figure 2 plots τ_w as we progressively remove these models, indicated on the horizontal axis. The rightmost points correspond to a setting with one model per family, containing only 7 of the initial 11 models.

Most SITE metrics exhibit a sharp drop in τ_w after ablation. Except on DTD and Pets, all SITE metrics fall below 0.6 once the oversized variants are removed. The results also show that none of the metrics are robust to changes in the model space. For every metric, a dataset exists where the removal of a single model results in a steep decrease in performance. In this more realistic setup, no metric reliably predicts transferability across datasets. This demonstrates that the high performance of these metrics is brittle and heavily reliant on correctly ranking a few over-represented models in a flawed benchmark. Most importantly, none of the existing SITE metrics are able to reliably estimate transferability in a setup where models of similar sizes are compared.

5.2 CRITIQUE 2: THE BENCHMARK IS SOLVED BY A STATIC RANKING

Dependencies between the candidate models (having larger and smaller variants of the same architecture in the model search space) and a lack of diversity in the evaluated datasets lead to a **static leaderboard**, where a few high-capacity models, such as ResNet-152, consistently occupy the top ranks regardless of the target dataset. We visualize the ranking of models in Figure 3. The figure shows that the top performing model, ResNet-152, occupies the first rank for 8 of the 10 datasets in the benchmark. The second place is always occupied by one of the top 3 models (ResNet-152, DenseNet-201, and ResNet-101).

As a result, we question whether the standard benchmark is suitable for assessing transferability estimation if a SITE metric with a data-independent ranking can achieve high-performance measurement. We probe this question by introducing a controlled experiment that tests whether a fixed, dataset-agnostic ranker can rival SITE metrics. This leads us to validate the hypothesis through

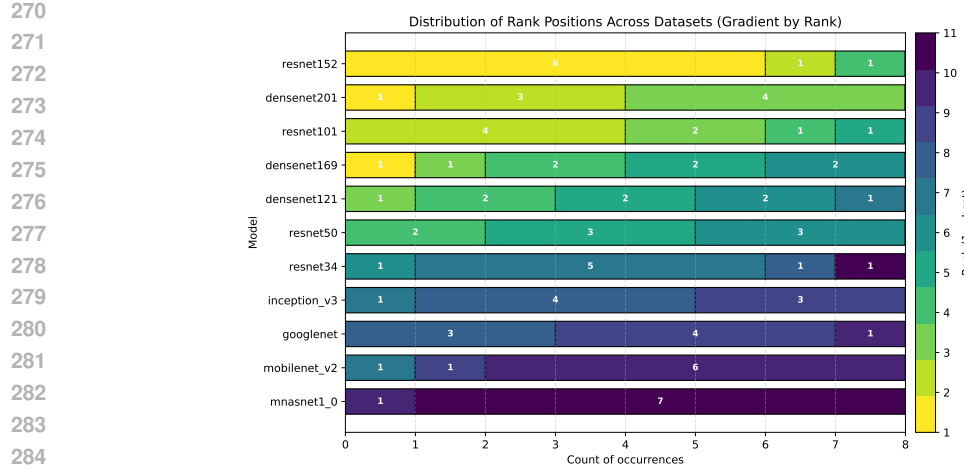


Figure 3: Visualization of the ranking distribution of models in the standard benchmark(ordered by fine tuned performance). The models at the top occupy the first ranks in most datasets.

Dataset Metric	Aircraft	CIFAR10	CIFAR100	DTD	Food	Pets	Average
GBC	-0.12	-0.02	0.09	0.14	0.10	-0.15	0.007
TransRate	0.14	0.51	0.20	0.20	-0.05	0.17	0.195
SFDA	-0.22	0.85	0.79	0.63	0.30	0.34	0.448
H-Score	0.60	0.91	0.80	0.04	0.59	0.37	0.552
NLEEP	-0.51	0.76	0.84	0.70	0.69	0.84	0.553
LogME	0.41	0.85	0.72	0.66	0.39	0.41	0.573
Static Ranking	0.84	0.91	0.98	0.99	0.80	0.94	0.91

Table 1: Comparison of transferability estimations, computed by weighted Kendall’s tau, for a static ranking versus SITE metrics on the standard benchmark. The static ranking achieves the highest τ_w overall.

a static ranker that exploits the leaderboard’s inherent bias without leveraging any task-specific information.

Validation via a Static Ranking Heuristic We test a naive **static ranker** in the standard benchmark, which orders models according to a fixed sequence. The static ranking follows a simple heuristic based on the model size and an alternation of ResNet and DenseNet model families, resulting in the following order:

ResNet-152>DenseNet-201>ResNet-101>DenseNet-169>ResNet-50>DenseNet-121>ResNet-34>GoogleNet>Inceptionv3>MobileNet>MNASNet.

We report the performance of this static ranking in Table 1. We observe that the static ranking significantly outperforms the sophisticated SITE metrics, achieving the highest τ_w on every dataset. On average, the static ranking achieves $\tau_w = 0.91$, while the best performing SITE metric, LogME, achieves $\tau_w = 0.57$. This finding questions the insight gained from the standard benchmark, as it rewards the memorization of a fixed model hierarchy rather than the ability to perform true task-specific transferability estimation.

5.3 CRITIQUE 3: SITE METRICS ARE NOT EVALUATED TOWARDS FIDELITY

Beyond ranking, a practical transferability metric should provide scores whose *magnitudes* are meaningful. That is, a large gap in metric scores should correspond to a large gap in downstream accuracy, allowing a user to assess whether selecting a higher-scoring model is worth the potential

increase in computational cost. The standard benchmark evaluation protocol, focused solely on rank correlation, overlooks this crucial property.

We formalize this property as follows. Let Δ_{Acc} be the difference in accuracy between two models on a target dataset \mathcal{D} , and let Δ_T be the difference in their transferability scores:

$$\Delta_{\text{Acc}}(X, Y; \mathcal{D}) = \text{Acc}(X, \mathcal{D}) - \text{Acc}(Y, \mathcal{D}), \quad \Delta_T(X, Y) = T(X) - T(Y)$$

An ideal metric should preserve the ordering of differences: for any four models A, B, C, D from the model space \mathcal{M} :

$$\forall A, B, C, D \in \mathcal{M}, \quad \Delta_{\text{Acc}}(A, B; \mathcal{D}) > \Delta_{\text{Acc}}(C, D; \mathcal{D}) \implies \Delta_T(A, B) > \Delta_T(C, D)$$

Validation via Pairwise Difference Correlation To quantify this property, which we term *fidelity to accuracy differences*, we formalize it as the correlation between pairwise differences in accuracy (Δ_{Acc}) and pairwise differences in the metric’s score (Δ_T). A high correlation would indicate that score differences are meaningful proxies for performance gaps.

We compute the Pearson correlation between all $\{\Delta_{\text{Acc}}\}$ and $\{\Delta_T\}$ pairs for each metric and dataset. The resulting heatmap is shown in Figure 4. We observe that nearly all metrics exhibit a weak correlation with accuracy differences. For example, our analysis reveals that a LogME score difference of 0.09 can correspond to an accuracy gap as large as 2.5% or as small as 0.5% in the Pets dataset. A more detailed plot of the relationships from scores to ground truth accuracies can be found in Appendix E. The lack of a reliable mapping between score gaps and performance gains severely limits the practical utility of these metrics for end-users, who cannot confidently interpret the scores to make informed decisions.

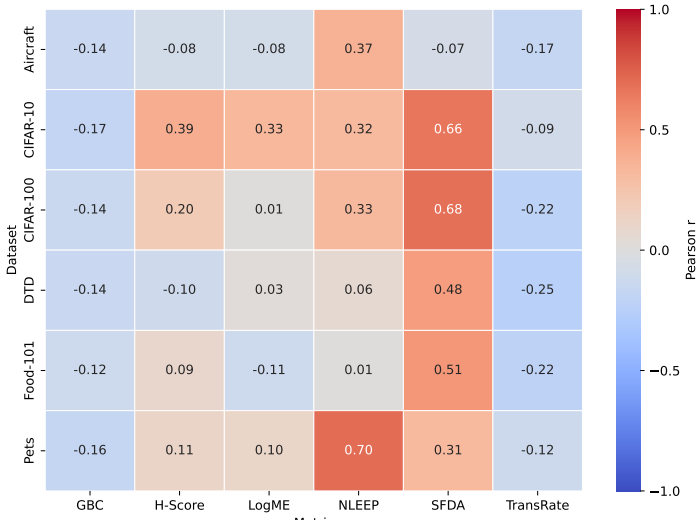


Figure 4: Heatmap correlation of Δ_{Acc} and Δ_T

5.4 TRANSFERABILITY ESTIMATION OUTSIDE OF COMPUTER VISION

In this work, we focus on popular computer vision and image classification setups; however, but other fields have similar benchmark issues. For example, MEAF (Hao & Wang, 2025) is a SITE metric for spiking neural networks, where our critique applies. The SEW-ResNet-152 model dominates the top rankings, and the performance differences can be as small as 0.2% at the second rank (which can occur due to fine-tuning differences). LogME experiments on NLP tasks also reveal one static winner every time as shown in Table 4. Critique 2, the comparison of models with varying sizes from the same families, can also be applied to recent work in object detection Zhang et al. (2025). Here, varying sizes of YOLO models were compared to one another for the same task, in which YOLOv5m won in 4 out of 5 tasks. EMMS (Meng et al., 2023) conducts an investigation into the transferability of ViT models while comparing ViT-S to ViT-B, where ViT-B outperforms every model and holds the first rank in 8 out of 11 tasks.

378

6 RELATED WORK

380 Previous work has conducted large-scale analysis of Source Independent Transferability Estimation
 381 (SITE) metrics. For instance, Agostinelli et al. (2022) perform a comprehensive evaluation across over
 382 700,000 experiments, showing that the effectiveness of a transferability metric is highly dependent
 383 on the specific experimental scenario. Although the setup proposed by Agostinelli et al. (2022) is
 384 thorough, its scale makes it impractical to reproduce in typical research settings without substantial
 385 computational resources. Similarly, Ibrahim et al. (2021) highlight the instability of SITE metrics in
 386 the presence of class imbalance and propose an adaptation of the H-score tailored to their setting.
 387 Baker & Handmann (2024) recommend different SITE metrics for different scenarios. Chaves et al.
 388 (2024), Kazemi et al. (2025), and Bolya et al. (2022) mention some drawbacks of the standard
 389 benchmark but continue to utilize an impractical model search space (Critique 1) and may encounter
 390 similar challenges as those associated with a static leaderboard (Critique 2). Kornblith et al. (2019)
 391 show that higher ImageNet accuracy predicts better transfer on web-scraped target datasets, which
 392 largely overlap with the datasets of the standard benchmark. Fang et al. (2023) demonstrate that this
 393 correlation breaks down for real-world datasets that are not web-scraped. Our work complements
 394 these findings by exposing dataset and model search space synergies that result in benchmark
 395 limitations.

396 In contrast to these studies, our goal is not to evaluate a particular SITE metric or to recommend
 397 which method to use and when, but rather to examine the benchmarks and recommend best practices
 398 for evaluating SITE metrics. We introduce a framework for assessing the effectiveness of SITE
 399 benchmarks and offer practical insights into constructing experimental setups that enable more
 400 reliable evaluations and better inform the practitioner, as the end use of these metrics is to provide
 401 improved evaluations for users.

402

7 DISCUSSION

403 In this section, we move from critique to construction and propose a set of actionable recommendations
 404 designed to foster the development of more robust and practically relevant benchmarks. We
 405 show how we can address the limitations identified in the previous section and move towards building
 406 a more reliable benchmark setup for SITE metrics. The goal is to ensure that future transferability
 407 metrics are validated against challenges that mirror the complexities faced by practitioners, thereby
 408 providing trustworthy guidance for real-world model selection. We therefore polish recommendations
 409 now on "How to build better benchmarks for your transferability estimation metric."

410 **Best Practice 1: Release code and data for your transferability estimation metric.**

411 In this work, we were only able to examine a handful of metrics and datasets due to the limitations
 412 of publicly available data. A good practice to ensure reproducibility and reduce noise in score
 413 discrepancies is to release the code for the metric, the datasets with links on which it was trained, the
 414 score metrics obtained, final accuracies, and the pretrained models on which the score was computed
 415 (for different task transfer scenarios). This, firstly, ensures full reproducibility and, secondly, allows
 416 for the incorporation of inconsistent scores in different works for the same task.

417 **Best Practice 2: Construct a Diverse and Non-Trivial Model Space**

418 To create a more robust evaluation, the model space must be intentionally diversified to present a
 419 non-trivial selection problem. This involves curating a set of models from **architecturally distinct**
 420 **paradigms**, such as Convolution Neural Networks (e.g., ConvNeXt), Vision Transformers (e.g., ViT,
 421 Swin), and MLP-based models (e.g., MLP-Mixer). Furthermore, to ensure a fair comparison that
 422 isolates the impact of architectural inductive bias, comparable models should be chosen **according to**
 423 **practitioners constraints, such as** computational budgets (e.g., parameter counts or FLOPs),**inference**
 424 **speed, training speed, etc.** This forces the evaluation of the metric to move beyond simple scaling rules
 425 and to make nuanced judgments about which architecture is best suited for the specific downstream
 426 task.

427 **Best Practice 3: Ensuring a Diverse and Challenging Dataset Space**

428 The suite of downstream tasks is as critical as the model space. A metrics utility is defined by its
 429 ability to generalize across a wide range of applications. A benchmark that relies on a narrow set of

similar or overly simplistic datasets cannot provide this assurance. We identify two essential axes of diversity for the dataset space:

- **Task Difficulty and Performance Headroom:** Many existing benchmarks use datasets where modern pre-trained models achieve near-saturated performance (e.g., 99% accuracy). This “performance ceiling” makes meaningful rankings impossible, as the marginal differences between top models are often statistically insignificant and fall within the noise of the fine-tuning process. A robust benchmark must include challenging datasets that provide sufficient performance headroom for even the strongest models, ensuring that a clear and statistically significant performance gap can be measured.
- **Domain and Task Variety:** A metric’s robustness is tested by its performance across varied domains and task types. **Consequently, the benchmark ought to incorporate datasets that cover a variety of visual domains, including fine-grained classification (for instance, FGVC Aircraft (Maji et al., 2013b), Stanford Cars (Krause et al., 2013)), medical imaging, satellite imagery, and texture analysis (such as DTD Cimpoi et al. (2014)).** Additionally, datasets that are not sourced from the internet should be included, consistent with the findings of Fang et al. (2023). This evaluates the metric’s capacity to handle varying degrees of domain shift from the original source pre-training data. We acknowledge that the property of diverse datasets is generally present in the majority of the SITE papers.

Best Practice 4: Engineering for Performance Spread and Rank Dispersion

A critical but often overlooked flaw in standard benchmarks is the persistence of a static model hierarchy, where one or two models dominate nearly all tasks. This “static leaderboard” undermines evaluation validity: a transferability metric can achieve a high weighted Kendall’s Tau simply by favoring the top model rather than by accurately predicting task-specific suitability. To isolate architectural inductive bias, models should be matched on computational budgets (e.g., parameter counts or FLOPs). This design forces transferability metrics to move beyond simple scaling laws and, instead, to make nuanced judgments about which architecture best fits a given task.

Equally important, an effective benchmark must exhibit high rank dispersion: model rankings should vary substantially across tasks, with different architectures excelling on different datasets. Achieving this requires a careful co-design of the model pool and dataset pool so that unique inductive biases are rewarded in different contexts. Such a setup provides a far more rigorous test of transferability metrics, ensuring they identify the right model for the right task rather than defaulting to the same top performer.

We view these guidelines as a first step toward evolving standards for benchmarking transferability estimation, which may need to adapt to different deployment settings, such as edge devices versus large-scale computing environments. **While our guidelines are essential steps, we also provide a benchmark for image classification that takes into account Best Practices 2,3, and 4 in the next section**

8 BENCHMARK BASED ON BEST PRACTICES

We built a robust benchmark based on the best practices described in the previous section. Our proposed benchmark consists of the following models: Twins-SVT (Chu et al., 2021), XCiT (El-Nouby et al., 2021), CoaT (Xu et al., 2021), DeiT (Touvron et al., 2021), MaxViT (Tu et al., 2022), and MViT v2 (Li et al., 2022). This selection covers complementary model design paradigms, while all models have a similar parameter range, and no model is a direct improvement over the other. Fine-tuning these selected models on datasets from the *standard benchmark* results in multiple models obtaining $> 99\%$ accuracy, which is not meaningful for SITE. To address this limitation, we expand the benchmark’s datasets with selected datasets from the Meta-Album (Ullah et al., 2022). From the 30 datasets of the Meta-Album, we do not select those where multiple models achieve very high or close to 100% accuracy.

Our resulting benchmark consists of the following datasets: Sports (Piosenka), Plant Village (G. & J., 2019), RESISC (Cheng et al., 2017), Insects (Wu et al., 2019), PanNuke (Gamper et al., 2019), MPII Human Pose Dataset (Andriluka et al., 2014), Fungi (Picek et al., 2021), RSD (Long et al., 2017), Boats (Gundogdu et al., 2017), Plant Doc (Singh et al., 2020), Stanford Actions (Yao et al., 2011), DTD (Cimpoi et al., 2014), Subcellular Human Protein Dataset(PRTA) (Thul et al., 2017), Insects

486 SPIPOLL (Wu et al., 2019), and Dogs Khosla et al. (2011). Based on Critique 2, we evaluate our
 487 benchmark against a static ranker. We create this static ranker based on the fine-tuned performance of
 488 models; more information on this can be found in the Appendix B.

489 We show the performance of SITE metrics and the static ranker on our benchmark in Table 2. We
 490 observe that not a single SITE metric can perform consistently well for our benchmark. The static
 491 ranker achieves comparably low values of $\tau_w \in [-0.3, 0.77]$ with a mean of 0.31. While following
 492 best practices, we propose that this benchmark should be used as an example to build a better and
 493 more reliable benchmark for SITE metric evaluation for different tasks, such as computer vision,
 494 NLP, and information retrieval.

Dataset	TransRate	LogME	NLEEP	SFDA	HScore	GBC	Static
Sports	0.39	0.25	0.30	0.70	-0.08	0.38	0.46
PlantVillage	0.18	0.61	0.61	-0.05	0.30	0.14	-0.30
RESISC	0.24	0.11	0.14	0.76	0.23	0.36	0.55
Stanford Actions	-0.16	-0.37	-0.28	-0.07	0.01	0.03	0.27
Insects	0.72	0.57	0.84	0.53	0.52	0.87	0.56
DTD	-0.53	-0.37	-0.37	-0.48	-0.33	-0.42	0.01
PanNuke	0.14	-0.06	0.24	0.68	0.13	0.40	0.00
Dogs	-0.71	-0.41	-0.62	-0.32	-0.30	-0.59	-0.15
MPII Human	0.34	0.27	0.25	0.18	0.24	0.23	0.50
Fungi	0.44	0.70	-0.22	0.77	0.40	0.34	0.77
Plant Doc	0.54	0.30	0.30	0.10	0.10	0.48	0.58
SPIPOLL	-0.15	0.10	-0.15	-0.28	-0.18	-0.15	0.32
RSD	0.02	-0.20	-0.34	-0.07	-0.06	-0.04	0.60
PTRA	0.28	-0.09	-0.44	0.14	0.38	0.29	0.37
Boats	0.20	-0.49	0.38	-0.32	-0.33	0.27	0.09
Average	0.13	0.061	0.04	0.15	0.06	0.17	0.31

510 Table 2: τ_w performance on 15 benchmark datasets from Meta-Album, showing the performance of
 511 LogME, SFDA, HScore, GBC, NLEEP, TransRate and Static Ranker.

515 9 LIMITATIONS AND FUTURE WORK

518 Our work examines the standard SITE benchmark for image classification; our investigation can serve
 519 as a blueprint for future studies in other setups and can be further expanded to NLP, object detection,
 520 and medical image classification domains as well. A limitation that current benchmarks and metrics
 521 suffer from is the integration of different finetuning strategies, optimizers, and hyperparameters in the
 522 SITE metric evaluation. Currently, the methods and benchmarks have not been developed to take
 523 these hyperparameters into account while predicting transferability, whereas research has shown that
 524 they play a significant role in model performance. **A promising direction can be the incorporation**
 525 **of learning from social choice theory (Zhang & Hardt, 2024) to improve the development of more**
 526 **reliable benchmarks for SITE.**

527 10 CONCLUSION

531 Benchmarking is the cornerstone of machine learning research, allowing researchers to develop
 532 robust ideas and enabling scientific progress. Without robust benchmarks, trust in research methods
 533 can erode; to prevent this, we have shown how to ground benchmarks in more realistic scenarios for
 534 SITE metrics. Our experiments highlighted critical failures in current benchmarking practices. To aid
 535 future research, we provide actionable best practices and a SITE benchmark and evaluation checklist
 536 for constructing robust benchmarks in the Appendix A, inspired by the NAS Checklist (Lindauer &
 537 Hutter, 2020). Our set of recommendations and proposed experiments is actionable and concrete,
 538 ensuring robust benchmarking of SITE metrics. This work serves as a call to action for the community
 539 to adopt more rigorous standards; by doing so, we can foster the development of transferability metrics
 that are genuinely useful to practitioners and provide truly predictive and reliable guidance.

540 11 REPRODUCIBILITY STATEMENT
541542 To enable reproducibility, we provide the code, data, and execution scripts in the supplementary files.
543 We also provide additional code for our experiments and Jupyter notebooks to reproduce the figures.
544545 546 REFERENCES
547548 Andrea Agostinelli, Michal Pandy, Jasper Uijlings, Thomas Mensink, and Vittorio Ferrari. How
549 stable are transferability metrics evaluations? In *Computer Vision – ECCV 2022: 17th European
550 Conference, Tel Aviv, Israel, October 23–27, 2022, Proceedings, Part XXXIV*, 2022. doi: 10.1007/
551 978-3-031-19830-4_18.552 Mykhaylo Andriluka, Leonid Pishchulin, Peter Gehler, and Bernt Schiele. 2d human pose estimation:
553 New benchmark and state of the art analysis. In *2014 IEEE Conference on Computer Vision and
554 Pattern Recognition*, pp. 3686–3693, 2014. doi: 10.1109/CVPR.2014.471.555 Nermeen Abou Baker and Uwe Handmann. One size does not fit all in evaluating model se-
556 lection scores for image classification. *Scientific Reports*, 14, 2024. URL <https://api.semanticscholar.org/CorpusID:274514229>.
557558 Yajie Bao, Yang Li, Shao-Lun Huang, Lin Zhang, Lizhong Zheng, Amir Zamir, and Leonidas Guibas.
559 An information-theoretic approach to transferability in task transfer learning. In *2019 IEEE
560 International Conference on Image Processing (ICIP)*, pp. 2309–2313, 2019. doi: 10.1109/ICIP.
561 2019.8803726.562 Daniel Bolya, Rohit Mittapalli, and Judy Hoffman. Scalable diverse model selection for accessible
563 transfer learning, 2022. URL <https://arxiv.org/abs/2111.06977>.
564565 Lukas Bossard, Matthieu Guillaumin, and Luc Van Gool. Food-101 – mining discriminative compo-
566 nents with random forests. In *European Conference on Computer Vision*, 2014.
567568 Lorenzo Bracciali, Anna Vettoruzzo, Prabhant Singh, Joaquin Vanschoren, Mohamed-Rafik
569 Bouguelia, and Nicola Conci. Meta-learning transformers to improve in-context generalization,
570 2025. URL <https://arxiv.org/abs/2507.05019>.
571572 Levy Chaves, Eduardo Valle, Alceu Bissoto, and Sandra Avila. Back to the basics on predicting
573 transfer performance, 2024. URL <https://arxiv.org/abs/2405.20420>.
574575 Zih-Ching Chen, Chao-Han Huck Yang, Bo Li, Yu Zhang, Nanxin Chen, Shuo-Yiin Chang, Rohit
576 Prabhavalkar, Hung yi Lee, and Tara Sainath. How to estimate model transferability of pre-trained
577 speech models? In *Interspeech 2023*, pp. 456–460, 2023. doi: 10.21437/Interspeech.2023-1079.578 Gong Cheng, Junwei Han, and Xiaoqiang Lu. Remote sensing image scene classification: Benchmark
579 and state of the art. *CoRR*, abs/1703.00121, 2017. URL <http://arxiv.org/abs/1703.00121>.
580581 Xiangxiang Chu, Zhi Tian, Bo Zhang, Xiaolin Wang, Chunhua Wei, Huaxia Xia, Jiange Shen, and
582 Chunhua Luo. Twins: Revisiting the design of spatial attention in vision transformers. In *Advances
583 in Neural Information Processing Systems (NeurIPS)*, 2021.
584585 Mircea Cimpoi, Subhransu Maji, Iasonas Kokkinos, Sammy Mohamed, and Andrea Vedaldi. De-
586 scribing textures in the wild. In *Proceedings of the IEEE Conference on Computer Vision and
587 Pattern Recognition (CVPR)*, June 2014.
588589 Jia Deng, Wei Dong, Richard Socher, Li-Jia Li, Kai Li, and Li Fei-Fei. Imagenet: A large-scale hier-
590 archical image database. In *2009 IEEE Conference on Computer Vision and Pattern Recognition*,
591 pp. 248–255, 2009. doi: 10.1109/CVPR.2009.5206848.592 Yuhe Ding, Bo Jiang, Aijing Yu, Aihua Zheng, and Jian Liang. Which model to transfer? a survey on
593 transferability estimation, 2024. URL <https://arxiv.org/abs/2402.15231>.

594 Alaaeldin El-Nouby, Hugo Touvron, Mathilde Caron, Piotr Bojanowski, Armand Joulin, Matthijs
 595 Douze, Ivan Laptev, Natalia Neverova, Gabriel Synnaeve, Jakob Verbeek, and Hervé Jegou. Xcit:
 596 Cross-covariance image transformers. In *Proceedings of the IEEE/CVF International Conference
 597 on Computer Vision (ICCV)*, 2021.

598 Alex Fang, Simon Kornblith, and Ludwig Schmidt. Does progress on imagenet transfer to real-world
 599 datasets? In *Thirty-seventh Conference on Neural Information Processing Systems Datasets and
 600 Benchmarks Track*, 2023. URL <https://openreview.net/forum?id=SS3CK3yx5Z>.

602 Geetharamani G. and Arun Pandian J. Identification of plant leaf diseases using a nine-layer deep
 603 convolutional neural network. *Computers and Electrical Engineering*, 76:323–338, 2019. ISSN
 604 0045-7906. doi: <https://doi.org/10.1016/j.compeleceng.2019.04.011>. URL <https://www.sciencedirect.com/science/article/pii/S0045790619300023>.

606 Jevgenij Gamper, Navid Alemi Koohbanani, Ksenija Benet, Ali Khuram, and Nasir Rajpoot. Pannuke:
 607 an open pan-cancer histology dataset for nuclei instance segmentation and classification. In
 608 *European Congress on Digital Pathology*, pp. 11–19. Springer, 2019.

610 Mohsen Gholami, Mohammad Akbari, Xinglu Wang, Behnam Kamranian, and Yong Zhang. Etran:
 611 Energy-based transferability estimation. In *Proceedings of the IEEE/CVF International Conference
 612 on Computer Vision*, pp. 18613–18622, 2023.

613 Erhan Gundogdu, Berkan Solmaz, Veysel Yucesoy, and Aykut Koc. Marvel: A large-scale image
 614 dataset for maritime vessels. In Shang-Hong Lai, Vincent Lepetit, Ko Nishino, and Yoichi Sato
 615 (eds.), *Computer Vision – ACCV 2016*, pp. 165–180, Cham, 2017. Springer International Publishing.
 616 ISBN 978-3-319-54193-8.

617 Haiqing Hao and Wenhui Wang. Bayesian transferability assessment for spiking neural net-
 618 works. *Transactions on Machine Learning Research*, 2025. ISSN 2835-8856. URL <https://openreview.net/forum?id=GaUtrgXMHe>.

621 Kaiming He, X. Zhang, Shaoqing Ren, and Jian Sun. Deep residual learning for image recognition.
 622 2016 IEEE Conference on Computer Vision and Pattern Recognition (CVPR), pp. 770–778, 2015.
 623 URL <https://api.semanticscholar.org/CorpusID:206594692>.

625 Andrew G. Howard, Menglong Zhu, Bo Chen, Dmitry Kalenichenko, Weijun Wang, Tobias Weyand,
 626 Marco Andreetto, and Hartwig Adam. Mobilenets: Efficient convolutional neural networks for
 627 mobile vision applications, 2017. URL <https://arxiv.org/abs/1704.04861>.

628 Zixuan Hu, Xiaotong Li, Shixiang Tang, Jun Liu, Yichun Hu, and Ling-Yu Duan. Lead: Exploring
 629 logit space evolution for model selection. In *2024 IEEE/CVF Conference on Computer Vision and
 630 Pattern Recognition (CVPR)*, 2024. doi: 10.1109/CVPR52733.2024.02708.

632 Gao Huang, Zhuang Liu, and Kilian Q. Weinberger. Densely connected convolutional networks.
 633 2017 IEEE Conference on Computer Vision and Pattern Recognition (CVPR), pp. 2261–2269,
 634 2016. URL <https://api.semanticscholar.org/CorpusID:9433631>.

635 Long-Kai Huang, Junzhou Huang, Yu Rong, Qiang Yang, and Ying Wei. Frustratingly easy trans-
 636 ferability estimation. In *International Conference on Machine Learning*, pp. 9201–9225. PMLR,
 637 2022.

639 Shibal Ibrahim, Natalia Ponomareva, and Rahul Mazumder. Newer is not always better: Rethinking
 640 transferability metrics, their peculiarities, stability and performance. In *ECML/PKDD*, 2021. URL
 641 <https://api.semanticscholar.org/CorpusID:238744475>.

642 Dovile Juodelyte, Enzo Ferrante, Yucheng Lu, Prabhant Singh, Joaquin Vanschoren, and Veronika
 643 Cheplygina. On dataset transferability in medical image classification, 2024. URL <https://arxiv.org/abs/2412.20172>.

646 Alireza Kazemi, Helia Rezvani, and Mahsa Baktashmotlagh. Benchmarking transferability: A
 647 framework for fair and robust evaluation, 2025. URL <https://arxiv.org/abs/2504.20121>.

648 Aditya Khosla, Nityananda Jayadevaprakash, Bangpeng Yao, and Li Fei-Fei. Novel dataset for
 649 fine-grained image categorization. In *First Workshop on Fine-Grained Visual Categorization, IEEE*
 650 *Conference on Computer Vision and Pattern Recognition*, Colorado Springs, CO, June 2011.

651

652 Simon Kornblith, Jonathon Shlens, and Quoc V. Le. Do better imagenet models transfer better? In
 653 *2019 IEEE/CVF Conference on Computer Vision and Pattern Recognition (CVPR)*, pp. 2656–2666,
 654 2019. doi: 10.1109/CVPR.2019.00277.

655 Jonathan Krause, Michael Stark, Jia Deng, and Li Fei-Fei. 3d object representations for fine-grained
 656 categorization. In *4th International IEEE Workshop on 3D Representation and Recognition*
 657 (*3dRR-13*), Sydney, Australia, 2013.

658 Alex Krizhevsky, Geoffrey Hinton, et al. Learning multiple layers of features from tiny images. 2009.

659

660 Xiaotong Li, Zixuan Hu, Yixiao Ge, Ying Shan, and Ling-Yu Duan. Exploring model transferability
 661 through the lens of potential energy. In *2023 IEEE/CVF International Conference on Computer*
 662 *Vision (ICCV)*, 2023. doi: 10.1109/ICCV51070.2023.00500.

663

664 Yandong Li, Xuhui Jia, Ruoxin Sang, Yukun Zhu, Bradley Green, Liqiang Wang, and Boqing Gong.
 665 Ranking neural checkpoints. In *2021 IEEE/CVF Conference on Computer Vision and Pattern*
 666 *Recognition (CVPR)*, 2021. doi: 10.1109/CVPR46437.2021.00269.

667

668 Yanghao Li, Chao-Yuan Wu, Haoqi Fan, Karttikeya Mangalam, Bo Xiong, Piotr Dollar, and Ross
 669 Girshick. Mvitv2: Improved multiscale vision transformers for classification and detection. In
 670 *Proceedings of the IEEE/CVF Conference on Computer Vision and Pattern Recognition (CVPR)*,
 671 2022.

672 Marius Lindauer and Frank Hutter. Best practices for scientific research on neural architecture
 673 search. *Journal of Machine Learning Research*, 21(243):1–18, 2020. URL <http://jmlr.org/papers/v21/20-056.html>.

674

675 Yang Long, Yiping Gong, Zhifeng Xiao, and Qing Liu. Accurate object localization in remote sensing
 676 images based on convolutional neural networks. *IEEE Transactions on Geoscience and Remote*
 677 *Sensing*, 55(5):2486–2498, 2017. doi: 10.1109/TGRS.2016.2645610.

678 Subhransu Maji, Esa Rahtu, Juho Kannala, Matthew B. Blaschko, and Andrea Vedaldi. Fine-grained
 679 visual classification of aircraft. *ArXiv*, abs/1306.5151, 2013a.

680 Subhransu Maji, Esa Rahtu, Juho Kannala, Matthew B. Blaschko, and Andrea Vedaldi. Fine-
 681 grained visual classification of aircraft. *ArXiv*, abs/1306.5151, 2013b. URL <https://api.semanticscholar.org/CorpusID:2118703>.

682

683 Fanqing Meng, Wenqi Shao, zhanglin peng, Chonghe Jiang, Kaipeng Zhang, Yu Qiao, and Ping
 684 Luo. Foundation model is efficient multimodal multitask model selector. In *Thirty-seventh*
 685 *Conference on Neural Information Processing Systems*, 2023. URL <https://openreview.net/forum?id=2ep5PXEZiw>.

686

687 Cuong V. Nguyen, Tal Hassner, Matthias Seeger, and Cedric Archambeau. Leep: a new measure
 688 to evaluate transferability of learned representations. In *Proceedings of the 37th International*
 689 *Conference on Machine Learning*, ICML’20. JMLR.org, 2020.

690

691 Omkar M. Parkhi, Andrea Vedaldi, Andrew Zisserman, and C. V. Jawahar. Cats and dogs. *2012*
 692 *IEEE Conference on Computer Vision and Pattern Recognition*, pp. 3498–3505, 2012. URL
 693 <https://api.semanticscholar.org/CorpusID:279027499>.

694

695 Lukas Picek, Milan Sulc, Jiri Matas, Jacob Heilmann-Clausen, Thomas S. Jeppesen, Thomas Laessoe,
 696 and Tobias Froslev. Danish fungi 2020 - not just another image recognition dataset. 2021.

697

698 Gerald Piosenka. 100 sports image classification. URL <https://www.kaggle.com/datasets/gpiosenka/sports-classification>.

699

700 Michal Pdy, Andrea Agostinelli, Jasper Uijlings, Vittorio Ferrari, and Thomas Mensink. Trans-
 701 ferability estimation using bhattacharyya class separability. In *2022 IEEE/CVF Conference on*
Computer Vision and Pattern Recognition (CVPR), 2022. doi: 10.1109/CVPR52688.2022.00896.

702 Christoph Schuhmann, Romain Beaumont, Richard Vencu, Cade W Gordon, Ross Wightman, Mehdi
 703 Cherti, Theo Coombes, Aarush Katta, Clayton Mullis, Mitchell Wortsman, Patrick Schramowski,
 704 Srivatsa R Kundurthy, Katherine Crowson, Ludwig Schmidt, Robert Kaczmarczyk, and Jenia
 705 Jitsev. LAION-5b: An open large-scale dataset for training next generation image-text models.
 706 In *Thirty-sixth Conference on Neural Information Processing Systems Datasets and Benchmarks*
 707 *Track*, 2022. URL <https://openreview.net/forum?id=M3Y74vmsMcY>.

708 Wenqi Shao, Xun Zhao, Yixiao Ge, Zhaoyang Zhang, Lei Yang, Xiaogang Wang, Ying Shan, and
 709 Ping Luo. Not all models are equal: Predicting model transferability in a self-challenging fisher
 710 space. In *Computer Vision – ECCV 2022: 17th European Conference, Tel Aviv, Israel, October*
 711 *23–27, 2022, Proceedings, Part XXXIV*, pp. 286–302, Berlin, Heidelberg, 2022. Springer-Verlag.
 712 ISBN 978-3-031-19829-8. doi: 10.1007/978-3-031-19830-4_17. URL https://doi.org.dianus.libr.tue.nl/10.1007/978-3-031-19830-4_17.

713 Davinder Singh, Naman Jain, Pranjali Jain, Pratik Kayal, Sudhakar Kumawat, and Nipun Batra.
 714 Plantdoc: A dataset for visual plant disease detection. In *Proceedings of the 7th ACM IKDD*
 715 *CoDS and 25th COMAD*, CoDS COMAD 2020, pp. 249–253, New York, NY, USA, 2020.
 716 Association for Computing Machinery. ISBN 9781450377386. doi: 10.1145/3371158.3371196.
 717 URL <https://doi.org/10.1145/3371158.3371196>.

718 Prabhant Singh, Yiping Li, and Yasmina Al Khalil. Analysis of transferability estimation metrics
 719 for surgical phase recognition. In *3rd Workshop in Data Engineering in Medical Imaging (DEMI)*
 720 *MICCAI Workshop 2025*, 2025.

721 Christian Szegedy, Wei Liu, Yangqing Jia, Pierre Sermanet, Scott E. Reed, Dragomir Anguelov,
 722 D. Erhan, Vincent Vanhoucke, and Andrew Rabinovich. Going deeper with convolutions. *2015*
 723 *IEEE Conference on Computer Vision and Pattern Recognition (CVPR)*, pp. 1–9, 2014.

724 Christian Szegedy, Vincent Vanhoucke, Sergey Ioffe, Jonathon Shlens, and Zbigniew Wojna. Rethink-
 725 ing the inception architecture for computer vision. *2016 IEEE Conference on Computer Vision and*
 726 *Pattern Recognition (CVPR)*, pp. 2818–2826, 2015. URL <https://api.semanticscholar.org/CorpusID:206593880>.

727 Mingxing Tan, Bo Chen, Ruoming Pang, Vijay Vasudevan, and Quoc V. Le. Mnasnet: Platform-aware
 728 neural architecture search for mobile. *2019 IEEE/CVF Conference on Computer Vision and Pattern*
 729 *Recognition (CVPR)*, pp. 2815–2823, 2018.

730 Yang Tan, Yang Li, and Shao-Lun Huang. Otce: A transferability metric for cross-domain cross-task
 731 representations. *2021 IEEE/CVF Conference on Computer Vision and Pattern Recognition (CVPR)*,
 732 2021.

733 Peter J Thul, Lovisa Akesson, Mikaela Wiking, Diana Mahdessian, Aikaterini Geladaki, Hammou
 734 Ait Blal, Tove Alm, Anna Asplund, Lars Bjork, and Lisa M Breckels. A subcellular map of the
 735 human proteome. *Science*, 356(6340), 2017.

736 Hugo Touvron, Matthieu Cord, Matthijs Douze, Francisco Massa, Alexandre Sablayrolles, and Hervé
 737 Jegou. Training data-efficient image transformers & distillation through attention. In *Proceedings*
 738 *of the 38th International Conference on Machine Learning (ICML)*, pp. 10347–10357, 2021.

739 Anh Tran, Cuong Nguyen, and Tal Hassner. Transferability and hardness of supervised classification
 740 tasks. In *2019 IEEE/CVF International Conference on Computer Vision (ICCV)*, pp. 1395–1405,
 741 2019. doi: 10.1109/ICCV.2019.00148.

742 Zhengzhong Tu, Hossein Talebi, Han Zhang, Feng Yang, Peyman Milanfar, Humphrey Shi, and
 743 Yinxiao Li. Maxvit: Multi-axis vision transformer. In *Proceedings of the European Conference on*
 744 *Computer Vision (ECCV)*, 2022.

745 Ihsan Ullah, Dustin Carrion, Sergio Escalera, Isabelle M Guyon, Mike Huisman, Felix Mohr, Jan N
 746 van Rijn, Haozhe Sun, Joaquin Vanschoren, and Phan Anh Vu. Meta-album: Multi-domain
 747 meta-dataset for few-shot image classification. In *Thirty-sixth Conference on Neural Information*
 748 *Processing Systems Datasets and Benchmarks Track*, 2022. URL <https://meta-album.github.io/>.

756 Sebastiano Vigna. A weighted correlation index for rankings with ties. In *Proceedings of the 24th*
 757 *International Conference on World Wide Web*, WWW '15, Republic and Canton of Geneva, CHE,
 758 2015. International World Wide Web Conferences Steering Committee. doi: 10.1145/2736277.
 759 2741088.

760 Zijian Wang, Yadan Luo, Liang Zheng, Zi Huang, and Mahsa Baktashmotagh. How far pre-trained
 761 models are from neural collapse on the target dataset informs their transferability. In *2023*
 762 *IEEE/CVF International Conference on Computer Vision (ICCV)*, 2023. doi: 10.1109/ICCV51070.
 763 2023.00511.

764 Xiaoping Wu, Chi Zhan, Yukun Lai, Ming-Ming Cheng, and Jufeng Yang. Ip102: A large-scale
 765 benchmark dataset for insect pest recognition. In *IEEE CVPR*, pp. 8787–8796, 2019.

766 Weijian Xu, Yifan Wang, Xizhou Zhang, Yue Cao, Kai Chen, Chunhua Shen, Han Hu, and Yichen
 767 Wei. Co-scale conv-attentional image transformers (coat). In *Proceedings of the IEEE/CVF*
 768 *International Conference on Computer Vision (ICCV)*, 2021.

769 Yuncheng Yang, Meng Wei, Junjun He, Jie Yang, Jin Ye, and Yun Gu. Pick the best pre-trained model:
 770 Towards transferability estimation for medical image segmentation. In Hayit Greenspan, Anant
 771 Madabhushi, Parvin Mousavi, Septimiu Salcudean, James Duncan, Tanveer Syeda-Mahmood, and
 772 Russell Taylor (eds.), *Medical Image Computing and Computer Assisted Intervention – MICCAI*
 773 2023, pp. 674–683, Cham, 2023. Springer Nature Switzerland.

774 Bangpeng Yao, Xiaoye Jiang, Aditya Khosla, Andy Lai Lin, Leonidas Guibas, and Li Fei-Fei. Human
 775 action recognition by learning bases of action attributes and parts. In *2011 International Conference*
 776 *on Computer Vision*, pp. 1331–1338, 2011. doi: 10.1109/ICCV.2011.6126386.

777 Kaichao You, Yong Liu, Mingsheng Long, and Jianmin Wang. Logme: Practical assessment of
 778 pre-trained models for transfer learning. In *International Conference on Machine Learning*, 2021.
 779 URL <https://api.semanticscholar.org/CorpusID:231985863>.

780 Guanhua Zhang and Moritz Hardt. Inherent trade-offs between diversity and stability in multi-task
 781 benchmarks. In *International Conference on Machine Learning*, 2024.

782 Tengxue Zhang, Yang Shu, Xinyang Chen, Yifei Long, Chenjuan Guo, and Bin Yang. Assessing
 783 pre-trained models for transfer learning through distribution of spectral components. *Proceedings*
 784 *of the AAAI Conference on Artificial Intelligence*, 39(21):22560–22568, Apr. 2025. doi: 10.
 785 1609/aaai.v39i21.34414. URL <https://ojs.aaai.org/index.php/AAAI/article/view/34414>.

786

787

788

789

790

791

792

793

794

795

796

797

798

799

800

801

802

803

804

805

806

807

808

809

810 SUPPLEMENTARY MATERIAL

812 A SITE BENCHMARK AND EVALUATION CHECKLIST

815 To aid future research, we provide a concrete checklist for constructing robust benchmarks inspired
 816 by NAS Checklist (Lindauer & Hutter, 2020)

817 Best practices for Building benchmark.

- 819 Ensure Diversity (Models should be from different families).
- 820 Match computational budgets (Models should be under similar parameter range).
- 821 Avoid Trivial hierarchies (Models should not be in incremental improvements over each other
 822 eg Inceptionv2, Inceptionv3, Inceptionv4) where one improvement is a proven improvement
 823 over other.
- 824 Include datasets with room for improvement. (Do not include datasets where all scores \geq
 825 99%).
- 826 Include datasets from multiple domains.
- 827 Engineer for rank dispersion (so different models win in different tasks) to avoid a static
 828 leaderboard. If this is not possible then examine if the following task requires transferability
 829 estimation.

831 Best practices for reporting experiments and evaluation

- 833 Report τ_w with ablation over every model.
- 834 Report correlation of Δ_T and Δ_{Acc}

836 Best practices for releasing code For all experiments you report, check if you released:

- 838 Code for the training pipeline used to evaluate the final architectures.
- 839 Code for computing SITE metric for specialized tasks as well like object detection and
 840 Regression.

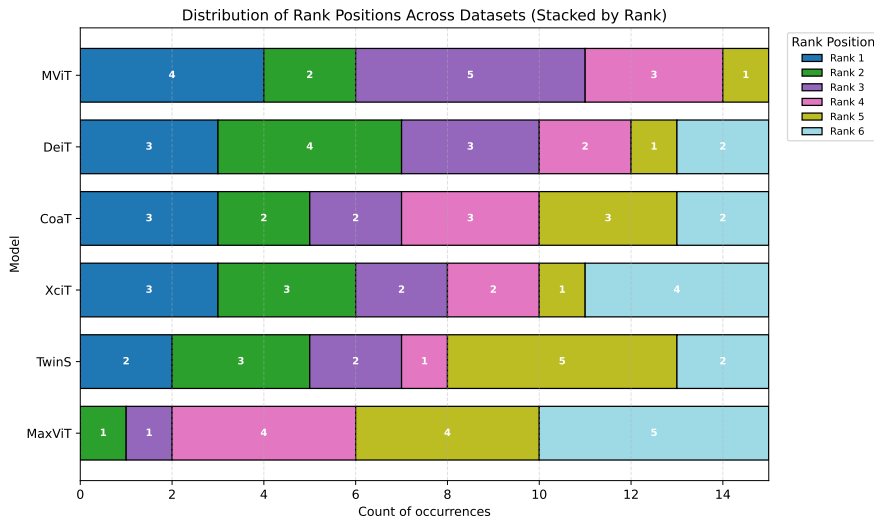
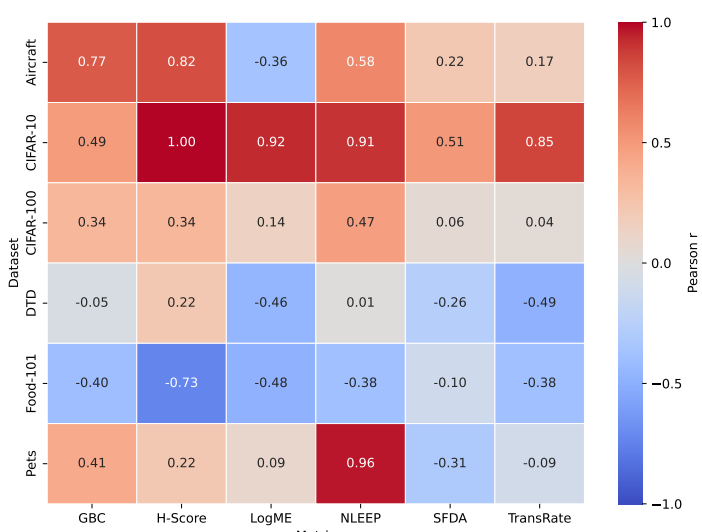
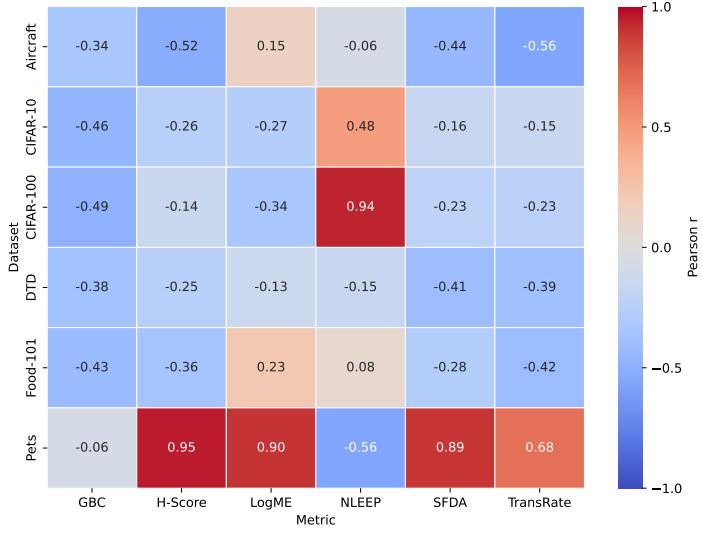
864 **B BENCHMARK BASED ON BEST PRACTICES**
865866 **B.1 STATIC RANKER**
867868 The final static ranking is determined by sorting the models based on these histograms. A model is
869 ranked higher if it has more first-place finishes. If two models have the same number of 1st place
870 finishes, the tie is broken by comparing their number of 2nd place finishes. This process continues
871 lexicographically through all rank positions, ensuring a stable and deterministic ordering.
872

Figure 5: Visualization of the ranking distribution of models in the improved benchmark. Most of the models share top spots and no model is always top or bottom rank.

893 **C ADDITIONAL ANALYSIS**
894895 **C.1 TOP-K MODELS ANALYSIS**
896897 The practical importance of fidelity is most pronounced when comparing top-performing models.
898 We therefore conducted a focused analysis on model pairs involving at least one from the top-3
899 ranks. The results show that even in this critical subset, the correlation between score gaps (Δ_T)
900 and accuracy gaps (Δ_{Acc}) remains weak and unreliable across all metrics. Large differences in
901 SITE scores between top-ranked models frequently corresponded to insignificant gaps in fine-tuned
902 accuracy, confirming that these metrics fail to provide meaningful guidance for selecting the best
903 model. This lack of fidelity for the most relevant models underscores their limited practical value for
904 real-world decision-making. We provide a detailed breakdown of this analysis in Figure 6 and Figure
905 7.
906907 **C.2 AGGREGATED PEARSON CORRELATION FOR METRIC FIDELITY**
908909 In Table 3, we list the average Pearson correlation of every metric between Δ_T and Δ_{Acc} , this metric
910 can be useful for practitioners to get a average idea of fidelity of different SITE metrics.
911912 **D LISTING FLAWED TABLES FROM PREVIOUS STUDIES**
913914 In Table 4 we can also observe that the RoBERTa model always outperforms other models, and
915 BERT-D always underperforms, which causes similar biases as discussed in our work. We observe
916 similar benchmark practices here, such as standard benchmarks with multiple different parameter
917 ranges of models coupled together and a static leaderboard.
918

Figure 6: Heatmap correlation of Δ_{Acc} and Δ_T for Top-4 ModelsFigure 7: Heatmap correlation of Δ_{Acc} and Δ_T for Bottom-4 models.

E SCORE VS ACCURACY FOR ALL SITE METRICS

We plot the SITE scores against the achieved ground truth accuracy to provide a more detailed picture of the fidelity of the scores to the differences in accuracy. Ideally, we observe a linear relationship such that we can infer from a large gap between scores a (comparatively) large gap between accuracies.

Figure 8 plots the GBC score against the accuracy. We observe that the distances between scores have no meaningful translation to the obtained accuracies. The majority of scores cluster in a very small range, and some outliers obtain visibly distinctive scores. Figure 9 shows that LogME is able to reflect meaningful distances in accuracy with its score for the CIFAR-10, and Cifar-100 and Food-101 datasets at least for the top performing models. This tendency is also observed in the correlation heatmap (cf. Figure 4). NLEEP indicates somewhat linear relationships for the CIFAR-10, CIFAR-100, Pets, and Food-101 dataset (cf. Figure 10). For the Aircraft dataset we observe an inverse relationship (the higher the score, the lower the accuracy). For SFDA (Figure 11), we can imagine

972 Table 3: Average Pearson correlation between accuracy differences and metric score differences
 973 across datasets
 974

Metric	Avg. Pearson r
SFDA	0.430
NLEEP	0.299
H-Score	0.101
LogME	0.047
GBC	-0.147
TransRate	-0.178

982
 983 Table 4: Original results from LogME NLP Experiments.
 984

task	RoBERTa	RoBERTa-D	uncased BERT-D	cased BERT-D	ALBERT-v1	ALBERT-v2	ELECTRA-base	ELECTRA-small	τ_w
MNLI	Accuracy	87.6	84.0	82.2	81.5	81.6	84.6	79.7	85.8
	LogME	-0.568	-0.599	-0.603	-0.612	-0.614	-0.594	-0.666	-0.621 0.66
QNLI	Accuracy	92.8	90.8	89.2	88.2	-	-	-	-
	LogME	-0.565	-0.603	-0.613	-0.618	-	-	-	- 1.00
SST-2	Accuracy	94.8	92.5	91.3	90.4	90.3	92.9	-	-
	LogME	-0.312	-0.330	-0.331	-0.353	-0.525	-0.447	-	- 0.68
CoLA	Accuracy	63.6	59.3	51.3	47.2	-	-	-	-
	LogME	-0.499	-0.536	-0.568	-0.572	-	-	-	- 1.00
MRPC	Accuracy	90.2	86.6	87.5	85.6	-	-	-	-
	LogME	-0.573	-0.586	-0.605	-0.604	-	-	-	- 0.53
RTE	Accuracy	78.7	67.9	59.9	60.6	-	-	-	-
	LogME	-0.709	-0.723	-0.725	-0.725	-	-	-	- 1.00

995 linear mappings that fit to most datasets. This is also reflected by comparatively large correlation
 996 between the SFDA score and the accuracy in Figure 4. Transrate’s scores are all over the place
 997 (cf. Figure 12), and the H-score exhibits some linear relationships for the Cifar-10, Cifar-100 and
 998 Food-101 datasets (cf. Figure 13).
 999

1000
 1001
 1002
 1003
 1004
 1005
 1006
 1007
 1008
 1009
 1010
 1011
 1012
 1013
 1014
 1015
 1016
 1017
 1018
 1019
 1020
 1021
 1022
 1023
 1024
 1025

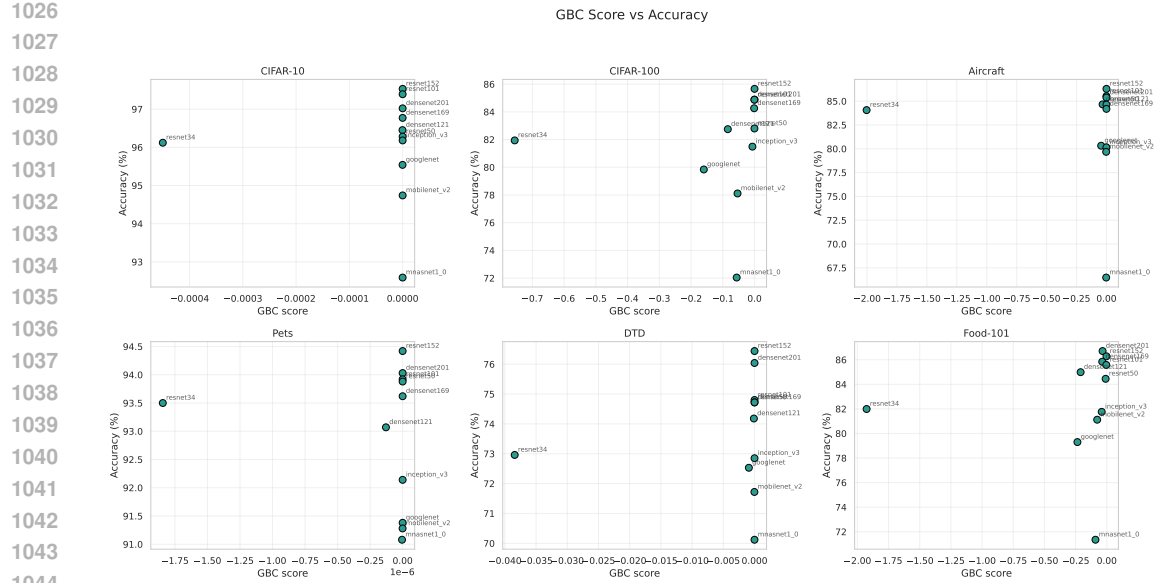


Figure 8: Plot of GBC scores against the ground truth accuracy.

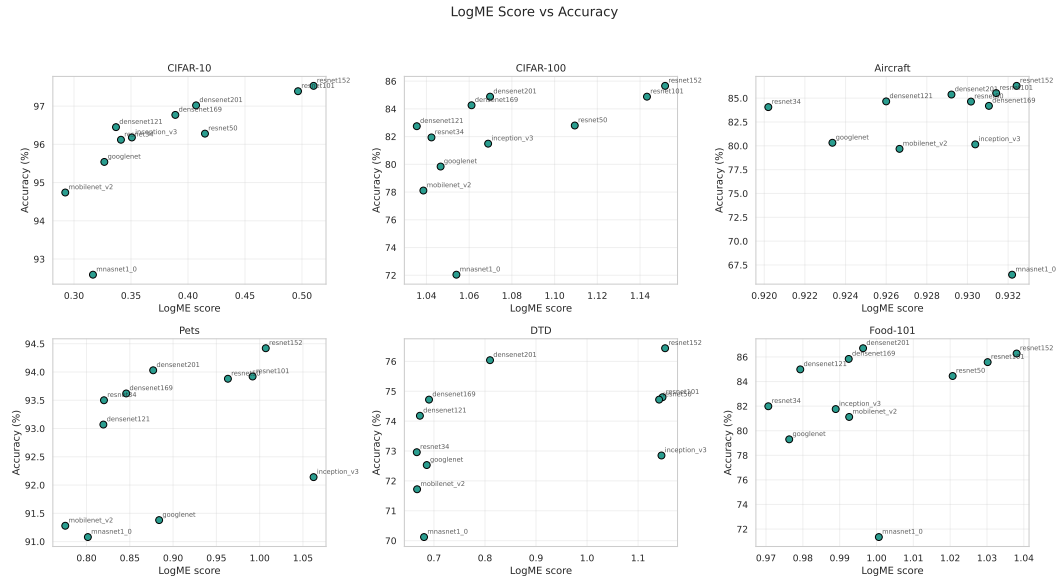


Figure 9: Plot of LogME scores against the ground truth accuracy.

F LLM USAGE

LLMs have been used for proofreading, and finding typos.

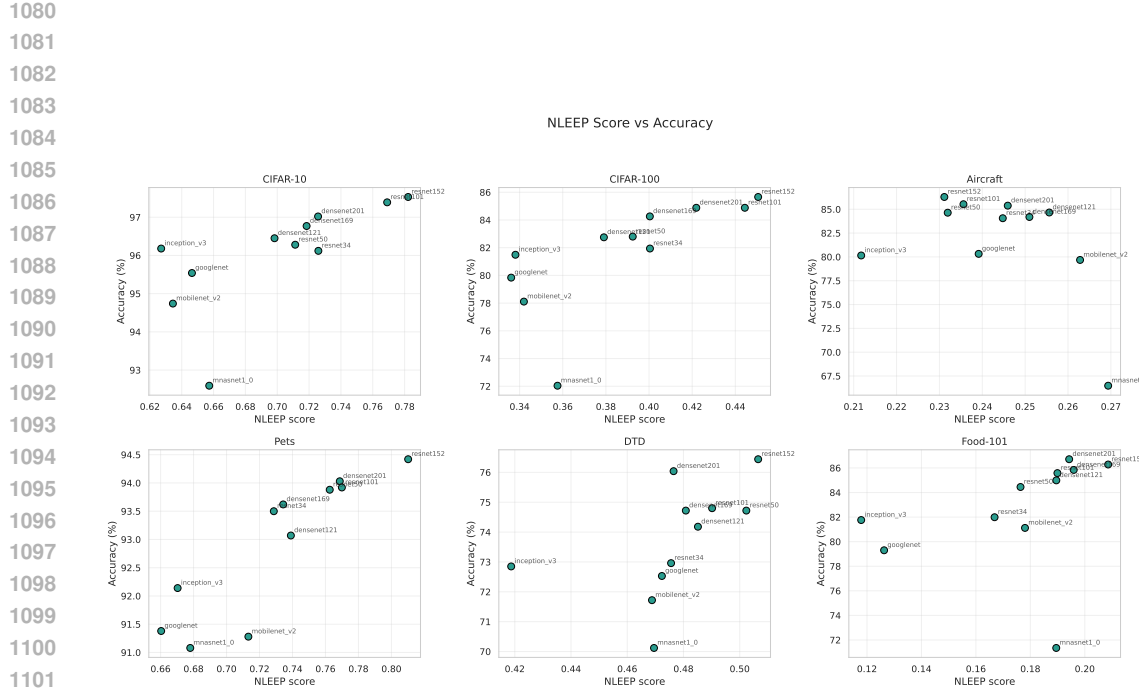


Figure 10: Plot of NLEEP scores against the ground truth accuracy.

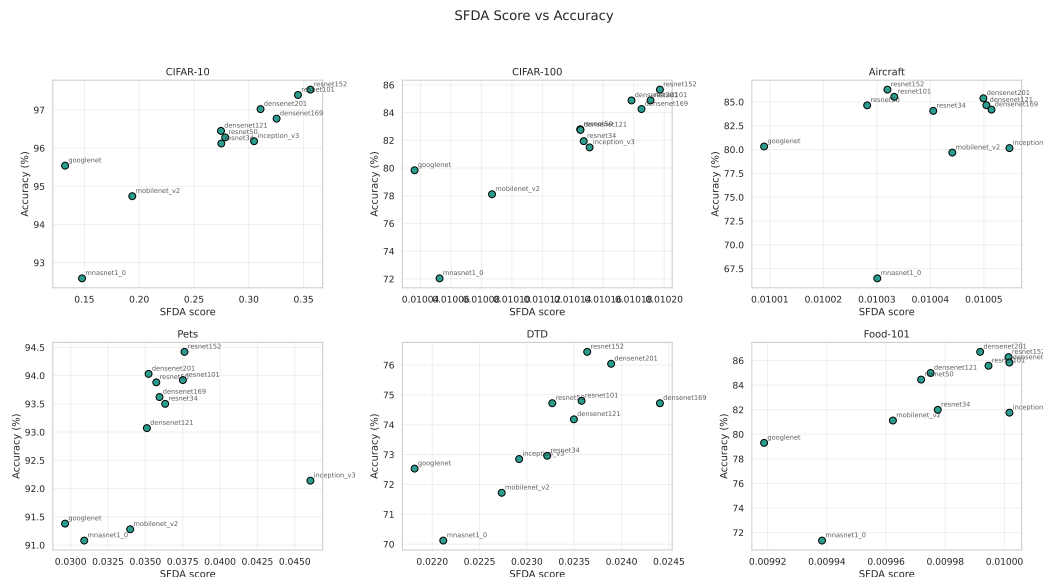


Figure 11: Plot of SFDA scores against the ground truth accuracy.

1134

1135

1136

1137

1138

1139

1140

1141

1142

1143

1144

1145

1146

1147

1148

1149

1150

1151

1152

1153

1154

1155

1156

1157

1158

1159

1160

1161

1162

1163

1164

1165

1166

1167

1168

1169

1170

1171

1172

1173

1174

1175

1176

1177

1178

1179

1180

1181

1182

1183

1184

1185

1186

1187

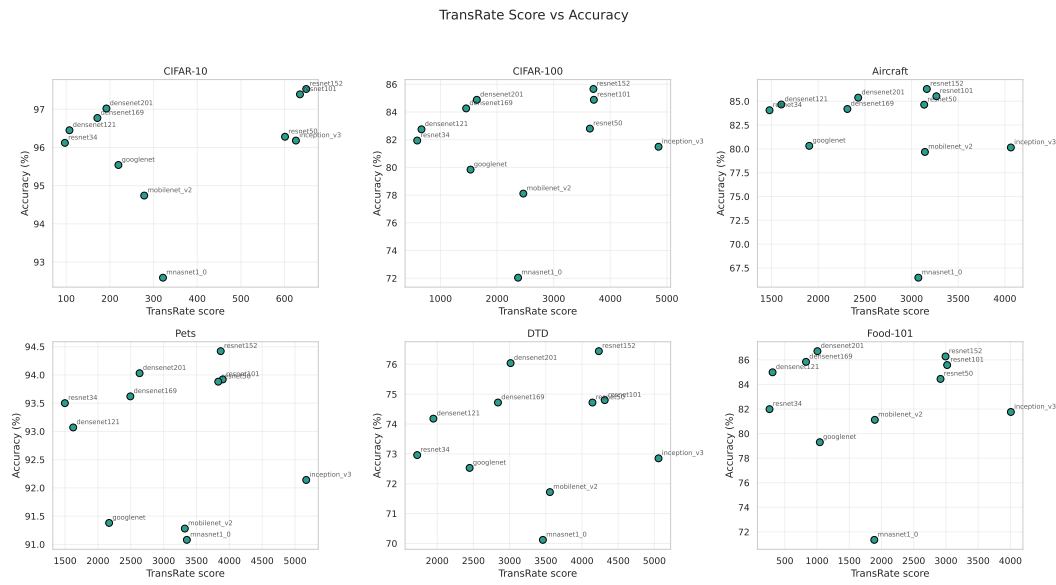


Figure 12: Plot of Transrate scores against the ground truth accuracy.

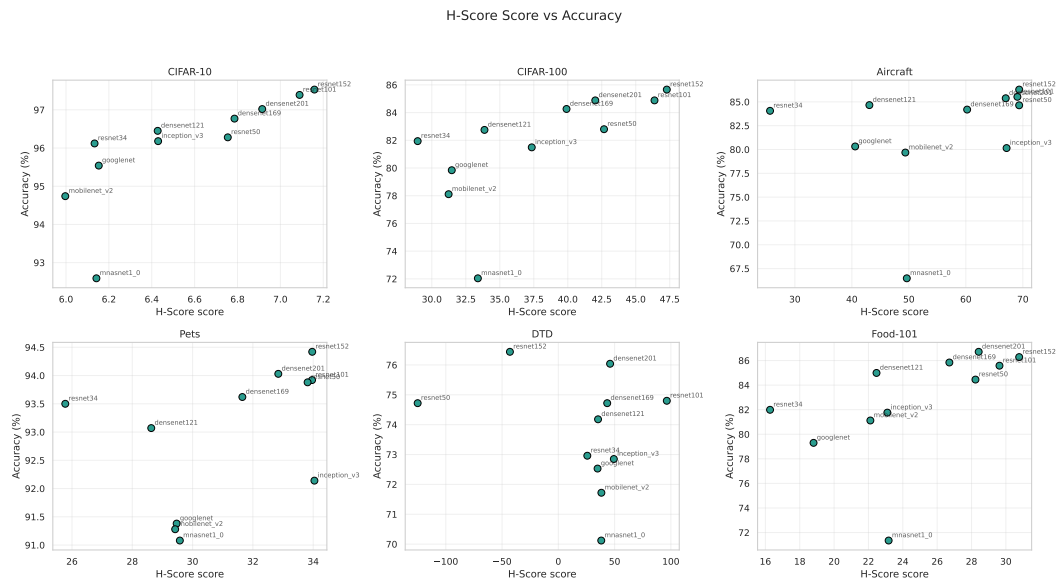


Figure 13: Plot of H-score against the ground truth accuracy.